Int. J. Solids Structures Vol. 16, pp. 119–130

0020-7683/80/1201-0119/$02.00/0

THE QUARTER-INFINITE CRACK IN A HALF SPACE; ALTERNATIVE AND ADDITIONAL SOLUTIONS

J. P. BENTHEM

Laboratory of Engineering Mechanics, Delft University of Technology, Mekelweg 2, 2628 CD Delft, The Netherlands

(*Received* 1 *November* 1978; *in revised form* 21 *March* 1979)

Abstract—Spherical coordinates are r, θ, ϕ. The half-space extends in $\theta < \pi/2$. The crack occurs along $\phi = 0$. In a previous paper in this journal *symmetrical* states of stress were considered in terms of the Cartesian stress components

$$\sigma_{xx} = r^{\lambda} f_{xx}(\lambda, \theta, \phi), \sigma_{xy} = r^{\lambda} f_{xy}(\lambda, \theta, \phi), \text{etc.}$$

which leave the half-space surface and the crack surfaces traction-free. Only a discrete spectrum of *eigenvalues* λ is possible and the most important λ-value is that closest to the limiting value Re $\lambda > -3/2$. The method followed was based on a separation of variables technique.

In present paper the results already obtained are confirmed by quite another method based on the use of finite differences. Some more information about the *eigenfunctions* i.e. the stresses is given. Now also the corresponding results for the *antimetrical* states of stress are evaluated.

1. INTRODUCTION

The quarter-infinite crack in a half-space is shown in Fig. 1. Cartesian coordinates are x, y, z, spherical coordinates r, θ, ϕ

$$\begin{aligned} x &= r \sin\theta \cos\phi \\ y &= r \sin\theta \sin\phi \\ z &= r \cos\theta. \end{aligned} \tag{1.1}$$

The half-space extends in $z > 0$. The crack occurs in the quarter-plane $y = 0$, $x > 0$, $z > 0$. The region to be investigated is a conical region (with vertex at $r = 0$) between the three planes

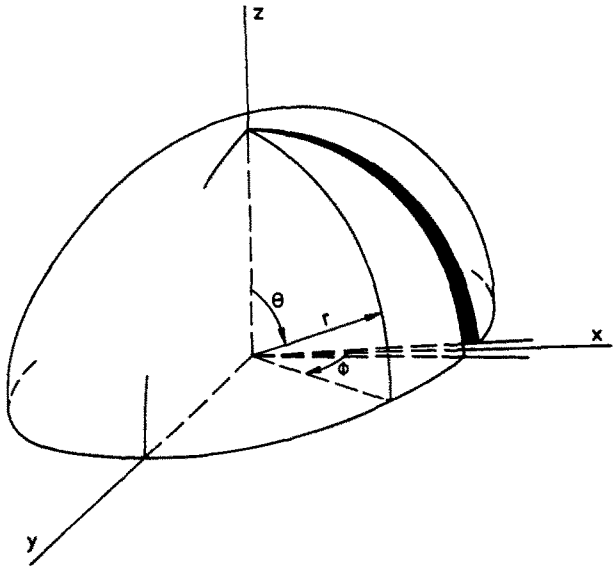

Fig. 1. The half-space $z > 0$ with the quarter-infinite crack $y = 0$, $x > 0$, $z > 0$. Cartesian coordinates x, y, z. Spherical coordinates r, θ, ϕ.

$\theta = \pi/2$, $\phi = +0$ and $\phi = 2\pi - 0$, which planes are to be taken traction-free. In this conical region a state of stress is considered in terms of the Cartesian stress-components

$$\sigma_{xx} = r^{\lambda} f_{xx}(\lambda, \theta, \phi), \sigma_{xy} = r^{\lambda} f_{xy}(\lambda, \theta, \phi), \text{etc.} \tag{1.2}$$

There is only a discrete spectrum of possible eigenvalues λ. The value λ which gives the most serious state of stress in the vertex region ($r \to 0$) is the value closest to the limiting value Re $\lambda > -3/2$.

In [1, 2] the author calculated λ values and corresponding states of stress (eigenfunctions) by a separation of variables technique, but only symmetrical states of stress were considered. The need was felt to confirm these results independently by quite another method. In some private correspondences and concept-papers kindly sent to the author the results of [1, 2] were questioned. Another reason was the fact that the separation of variables technique is not suitable for future applications to oblique cracks in the half-space. Therefore a finite difference method was applied. Of course in the first place the symmetrical states of stress of the quarter-infinite crack (orthogonal to the half-space surface) were reanalysed. The agreement was quite fair.

The corresponding results for the antimetrical states of stress, now given by the finite difference method, are believed to be still somewhat more accurate for a reason to be explained.

2. EXISTENCE OF THE EIGENFUNCTIONS

It has been known since a long time that two-dimensional wedges in plain strain with homogeneous boundary conditions have an infinite enumerable number of eigenvalues λ and eigenfunctions

$$\sigma_{xx} = r^{\lambda} f_{xx}(\lambda, \phi), \text{etc.}$$

where r, ϕ are polar coordinates. The eigenvalues λ occur in the complex λ-plane on or in pairs at both sides close to the real axis. The mean density of these eigenvalues is constant all along that real axis.

In [3] it has been proved that this is also true for the eigenvalues λ and eigenfunctions (1.2) for conical regions. The mean density of the λ-values is however not constant but proportional to $|\text{Re}\,\lambda|$ as is explained in [1]. Compare also the discussion in [4], pp. 753–762 on the eigenfrequencies and modes of vibration of a membrane.

A conical region will always be only a part of a finite configuration. In order that the strain energy be finite in the neighbourhood of the vertex, only eigenfunctions with

$$\text{Re}\,\lambda > -3/2\dagger \tag{2.1}$$

can occur there and thus we are not interested in eigenvalues and their eigenfunctions with Re $\lambda < -3/2$.‡ The eigenvalue with real part greater than $-3/2$, but closest to this value, will be called the gravest eigenvalue and its eigenfunction of displacements and stresses the gravest eigenfunction.

The present region under investigation has of course a very simple geometrical structure and one could ask if it is not possible to give the eigenfunctions a closed form. Symmetrical eigenfunctions are for all Poisson's ratio's ν

$(\lambda = -1)$ Two rigid body translations.

$\lambda = 0$ A rigid body rotation

and

$\sigma_{xx} = \text{constant}$.

†This means one should tolerate, if necessary, within the framework of linear elasticity theory, displacements $u \sim r^{\gamma}$, Re $\gamma > -1/2$, that become infinite at the vertex. But until now, no conical configurations with such a strong singularity ($0 > \text{Re}\,\gamma > -1/2$) are known.

‡In [3] it has been proved that if λ is an eigenvalue, also $-\lambda - 3$ is an eigenvalue. (Note in [3] the symbol λ has another meaning.)

$$\lambda = 1 \quad \sigma_{xx} = z.$$

$$\sigma_{xx} = x, \sigma_{xy} = -y.$$

$$\sigma_{xx} = x, \sigma_{xz} = -z.$$

$$\lambda = 2 \quad \sigma_{xx} = -2(1+\nu)xz, \sigma_{xy} = 2\nu yz, \sigma_{xz} = z^2.$$

$$\left.\begin{aligned} \sigma_{xx} &= -(1+\nu)x^2 + (2+\nu)y^2, \sigma_{xy} = (2+\nu)xy, \\ \sigma_{yy} &= -y^2, \sigma_{zx} = \nu xz, \sigma_{zy} = -\nu yz \end{aligned}\right\}$$

and at all further $\lambda = 3, 4, 5 \ldots\ldots$ there are other triple or double polynomial solutions.

Antimetrical eigenfunctions are

($\lambda = -1$) A rigid body translation.
($\lambda = 0$) Two rigid body rotations.

$$\lambda = 1 \quad \sigma_{xx} = y.$$

$$\lambda = 2 \quad \sigma_{xx} = -2(1+\nu)xy, \sigma_{xy} = y^2, \sigma_{zx} = 2\nu yz$$

and at all $\lambda = 1/2, 3/2, 5/2, \ldots\ldots$ there are (single) eigenfunctions

$$\begin{aligned} \sigma_{xx} &= r^\lambda\{-(4+4\nu+\lambda)\cos\lambda\phi + \lambda\cos(\lambda-2)\phi\}(\sin\theta)^\lambda \\ \sigma_{xy} &= r^\lambda\{(2+2\nu+\lambda)\sin\lambda\phi - \lambda\sin(\lambda-2)\phi\}(\sin\theta)^\lambda \\ \sigma_{yy} &= r^\lambda\{\lambda\cos\lambda\phi - \lambda\cos(\lambda-2)\phi\}(\sin\theta)^\lambda \\ \sigma_{zx} &= 2r^\lambda\nu\lambda\cos(\lambda-1)\phi\cos\theta(\sin\theta)^{\lambda-1} \\ \sigma_{zy} &= -2r^\lambda\nu\lambda\sin(\lambda-1)\phi\cos\theta(\sin\theta)^{\lambda-1} \\ \sigma_{zz} &= 0. \end{aligned} \tag{2.2}$$

Also integral values $\lambda = 0, 1, 2, 3, \ldots\ldots$ are allowed in (2.2) but then symmetrical eigenfunctions arise which are included among those already mentioned. In spite of fulfilment of requirement (2.1) the values $\lambda = -1/2$ (if $\nu \neq 0$) and $\lambda = -1$ are forbidden in (2.2) because the strain energy should become non-integrable along the entire crack-front ($\theta = 0$).

It is obvious that the aforementioned eigenfunctions are not all eigenfunctions (with Re $\lambda > -3/2$). The mean density of their eigenvalues along the real λ-axis would be only constant and not proportional to $|\mathrm{Re}\,\lambda|$ and the density of the symmetrical ones would be greater than the density of the antimetrical ones. The other eigenfunctions cannot be given expressions in closed form and they must be determined numerically. To those belong the gravest ones in which we are primarily interested. The mere increasing density of the eigenvalues is however prohibitive for the determination of many of them and their eigenfunctions in any numerical way.

3. CHOICE OF THE NUMERICAL METHOD

In search for the eigenvalues λ and their eigenfunctions the equations of elasticity theory need only to be applied to the demispherical surface $r = 1$, because along a certain radius all stresses are proportional to r^λ, all displacements to $r^{\lambda+1}$. On the surface $r = 1$ the range of the two remaining coordinates is

$$0 < \theta \leq \pi/2, 0 \leq \phi \leq 2\pi. \tag{3.1}$$

Determination of an eigenvalue resembles the determination of an eigenfrequency of a two-dimensional structure, e.g. a demi-spherical shell (λ playing the rôle of a frequency).

In [1, 2] a separation of variables (θ, ϕ) was applied. This means that the differential equations in question are exactly satisfied within the range (3.1), but conditions on boundaries of the range (3.1) only approximately. Application of a finite element method or a finite difference method means that the equations in question are everywhere only satisfied approximately. Moreover the number of unknowns to be solved simultaneously will be about the square of the number of unknowns from a separation of variables technique.

Bažant and Estenssoro [5, 6], have developed for conical regions a finite element method and applied it to a crack in a half-space. Where the present range of the coordinates is so very simple the method of finite differences is of course readily available. Only the governing differential equations need to be transformed into finite difference equations. It is true that the boundary equations are more complicated than at the finite element method and tend to broaden the band-width of the matrix of the coefficient of the unknowns. On the other hand these more complicated equations strengthen considerably the convergence of the numerical procedure.

4. DIFFERENTIAL EQUATIONS

The differential equations of elasticity theory will be expressed for *Cartesian* displacement—and stress-components as functions of *curvilinear* coordinates. By that means the displacement-components have only a scalar character, their derivatives only a vector character. The curvilinear coordinates are the spherical coordinates of (1.1) with however the polar angle θ replaced by ζ

$$\begin{aligned} &\theta = \zeta^2 \\ &0 < \zeta \leq \sqrt{(\pi/2)}. \end{aligned} \tag{4.1}$$

On the sphere $r = 1$, starting from $\theta = 0$, along a coordinate-line $\phi =$ constant, displacements show a series development

$$u = c_0 + c_1\theta^{1/2} + c_2\theta + c_3\theta^{3/2} + c_4\theta^2 + c_5\theta^{5/2} + \ldots\ldots .$$

By introduction of the new coordinate ζ of (4.1) the displacements become a regular function of that coordinate. The coordinate transformation formulas thus become

$$\begin{aligned} x &= r \sin\zeta^2 \cos\phi \\ y &= r \sin\zeta^2 \sin\phi \\ z &= r \cos\zeta^2 \end{aligned} \tag{4.2}$$

and the transformation-matrices of the partial differential quotients are†

$$T_\alpha^i = \left\| \begin{matrix} \frac{\partial x}{\partial r} & \frac{\partial x}{\partial \zeta} & \frac{\partial x}{\partial \phi} \\ \frac{\partial y}{\partial r} & \frac{\partial y}{\partial \zeta} & \frac{\partial y}{\partial \phi} \\ \frac{\partial z}{\partial r} & \frac{\partial z}{\partial \zeta} & \frac{\partial z}{\partial \phi} \end{matrix} \right\| = \left\| \begin{matrix} \sin\zeta^2\cos\phi & 2r\zeta\cos\zeta^2\cos\phi & -r\sin\zeta^2\sin\phi \\ \sin\zeta^2\sin\phi & 2r\zeta\cos\zeta^2\sin\phi & r\sin\zeta^2\cos\phi \\ \cos\zeta^2 & -2r\zeta\sin\zeta^2 & 0 \end{matrix} \right\| \tag{4.3}$$

$$t_i^\alpha = \left\| \begin{matrix} \frac{\partial r}{\partial x} & \frac{\partial r}{\partial y} & \frac{\partial r}{\partial z} \\ \frac{\partial \zeta}{\partial x} & \frac{\partial \zeta}{\partial y} & \frac{\partial \zeta}{\partial z} \\ \frac{\partial \phi}{\partial x} & \frac{\partial \phi}{\partial y} & \frac{\partial \phi}{\partial z} \end{matrix} \right\| = \left\| \begin{matrix} \sin\zeta^2\cos\phi & \sin\zeta^2\sin\phi & \cos\zeta^2 \\ \frac{1}{2r\zeta}\cos\zeta^2\cos\phi & \frac{1}{2r\zeta}\cos\zeta^2\sin\phi & -\frac{1}{2r\zeta}\sin\zeta^2 \\ -\frac{1}{r}\frac{\sin\phi}{\cos\zeta^2} & \frac{1}{r}\frac{\cos\phi}{\sin\zeta^2} & 0 \end{matrix} \right\| . \tag{4.4}$$

†Latin indices refer to x, y, z. Greek indices to r, ζ, ϕ.

The metric tensors of the r, ζ, ϕ system are

$$g_{\alpha\beta} = \delta_{ij} T_\alpha^{\ i} T_\beta^{\ j} \tag{4.5}$$

$$g^{\alpha\beta} = \delta^{ij} t_i^{\ \alpha} t_j^{\ \beta} \tag{4.6}$$

and the Christoffel symbols (the not mentioned are zero)

$$\begin{aligned} &\Gamma_{22}^1 = -4r\zeta^2, \Gamma_{33}^1 = -r(\sin\zeta^2)^2, \\ &\Gamma_{12}^2 = \Gamma_{21}^2 = \frac{1}{r}, \Gamma_{33}^2 = -\frac{1}{2\zeta}\sin\zeta^2\cos\zeta^2, \\ &\Gamma_{13}^3 = \Gamma_{31}^3 = \frac{1}{r}, \Gamma_{23}^3 = \Gamma_{32}^3 = 2\zeta\cot\zeta^2, \\ &\Gamma_{22}^2 = \frac{1}{\zeta}. \end{aligned} \tag{4.7}$$

The Cartesian stress components are σ_j^i, the Cartesian displacement components are u_i. All differentiations are partial with respect to the curvilinear coordinates r, ζ, ϕ and indicated by a comma.

The relation between stresses and displacement-derivatives becomes (the stress–strain relations, G is shear modulus, ν Poisson's ratio, $\nu \neq 1/2$)

$$\sigma_j^i = G\left(\frac{2\nu}{1-2\nu}\delta_j^i\delta^{km} + \delta^{ik}\delta_j^m + \delta^{im}\delta_j^k\right) t_m^{\ \alpha} u_{k,\alpha}. \tag{4.8}$$

The Navier–Cauchy equations are ($\eta = 1, 2, 3$; $\nu \neq 1/2$)

$$\{(1-2\nu)g^{\alpha\beta}\delta_\eta^{\ \gamma} + g^{\alpha\gamma}\delta_\eta^{\ \beta}\} T_\gamma^{\ i}(u_{i,\alpha\beta} - u_{i,\sigma}\Gamma_{\alpha\beta}^{\sigma}) = 0. \tag{4.9}$$

Due to the mixed Cartesian-curvilinear approach the transformation matrices (4.3) and (4.4) still occur in (4.8) and (4.9), but this has the great advantage that no multiplications and differentiations of Christoffel symbols are needed.

5. FINITE DIFFERENCE EQUATIONS

The "rectangular" ζ, ϕ range

$$0 < \zeta \leq \sqrt{(\pi/2)}; 0 \leq \phi \leq 2\pi \tag{5.1}$$

is divided in $M \times N$ equal meshes $\Delta\zeta$, $\Delta\phi$. The mesh lines in ϕ direction are numbered $\alpha = 0, 1, 2 \ldots M$, the mesh lines in ζ direction $\beta = 0, 1, 2 \ldots N$. As unknowns of the problem next to the eigenvalue λ are chosen the three Cartesian displacement components u_i in the nodal points

$$\begin{aligned} &\alpha = 1, 2, \ldots M-1, \beta = 0, 1 \ldots N \\ \text{and} \quad &\alpha = M, \beta = 1, 2, \ldots N-1. \end{aligned} \tag{5.2}$$

The boundary conditions expressing that the appropriate three stresses (tractions) σ_j^i from (4.8) are zero are applied to the nodal points

$$\begin{aligned} &\alpha = 1, 2, \ldots M-1, \beta = 0 \text{ and } N \\ &\alpha = M, \beta = 1, 2 \ldots N-1 \end{aligned} \tag{5.3}$$

and the Navier–Cauchy eqns (4.9) to the remaining nodal points of (5.2).

Because along a certain radius all u_i behave like $r^{\lambda+1}$ all differentiations in r-direction are still performed analytically. In ζ - and ϕ-direction 5-points differention rules were applied. If $y_0, y_1 \ldots y_4$ are values of a function $y = f(x)$ at 5 stations $x = x_0, x_1 \ldots x_4$ at equal distances h, these rules are

$$\text{at } x = x_0, \frac{dy}{dx} = \frac{1}{12h}(-25y_0 + 48y_1 - 36y_2 + 16y_3 - 3y_4) + 0(h^4 y^v)$$

$$x = x_1, \frac{dy}{dx} = \frac{1}{12h}(-3y_0 - 10y_1 + 18y_2 - 6y_3 + y_4) + 0(h^4 y^v)$$

$$x = x_2, \frac{dy}{dx} = \frac{1}{12h}(y_0 - 8y_1 + 8y_3 - y_4) + 0(h^4 y^v)$$

$$x = x_0, \frac{d^2y}{dx^2} = \frac{1}{12h^2}(35y_0 - 104y_1 + 114y_2 - 56y_3 + 11y_4) + 0(h^3 y^v)$$

$$x = x_1, \frac{d^2y}{dx^2} = \frac{1}{12h^2}(11y_0 - 20y_1 + 6y_2 + 4y_3 - y_4) + 0(h^3 y^v)$$

$$x = x_2, \frac{d^2y}{dx^2} = \frac{1}{12h^2}(-y_0 + 16y_1 - 30y_2 + 16y_3 - y_4) + 0(h^4 y^{vi}).$$

The error of these rules is only proportional to h^3 or h^4. The use of more points broadens the bandwidth of the matrix of the coefficients of the unknowns. Less points ask more meshes and thus more unknowns. After numerical experiments it was decided to use the aforementioned 5-point rules and the majority of the computations were performed with $M = 10$, $N = 30$.

The number of the equations is $3(MN + M - 2)$. They have all zero right hand sides. By a rather easy trial and error procedure a value of λ is sought that makes the governing determinant zero. As is explained in [1, 2], the search had to be carried out only for real values of λ. Next to the combination $M \times N = 10 \times 30$ in some cases also combinations 8×24, 12×36, 14×42, 16×48 were tried. The convergence showed that generally the gravest exponent λ had already an accuracy in 3 or 4 digits at the use of $M \times N = 10 \times 30$. The displacements may have an error of 1%, the stresses of some 3% of the maximum values. In [5, 6], where a finite element method was applied, the convergence of the λ-values was much less but final λ-values could be produced by an extrapolation procedure to $M, N \to \infty$. (In [5, 6] displacements were not given and stresses not computed).

6. SPECIALIZATION FOR THE INCOMPRESSIBLE MEDIUM

For ν values that tend to 1/2, the eqns (4.8) and (4.9) need to be transformed such that they also endure the value $\nu = 1/2$. To this purpose a further unknown

$$p = \frac{1}{3}\sigma_i^i \tag{6.1}$$

is introduced in all nodal points. The replacement for (4.8) is

$$\sigma_j^i = \frac{3\nu}{1+\nu} p\delta_j^i + G(\delta^{ik}\delta_j^m + \delta^{im}\delta_j^k) t_m^{\alpha} u_{k,\alpha} \tag{6.2}$$

and the three ($\eta = 1, 2, 3$) eqns (4.9) are replaced by the four ones

$$g^{\alpha\beta} T_\eta^i (u_{i,\alpha\beta} - u_{i,\sigma}\Gamma_{\alpha\beta}^{\sigma}) + \frac{3}{2(1+\nu)G} p_{,\eta} = 0 \tag{6.3}$$

$$\delta^{ij}u_{i,\alpha}t_j^{\alpha} - \frac{3(1-2\nu)}{2(1+\nu)G}p = 0. \tag{6.4}$$

The eqn (6.2) was applied to the nodal points (5.3) such that three tractions are zero, the eqns (6.3) to the remaining nodal points and the eqn (6.4) to all nodal points (5.2). To avoid singular behaviour of the unknowns p at $\zeta \to 0$ (it is of order $\zeta^{-1} = \theta^{-1/2}$) they are replaced by $p\zeta$. The special computer programme based on (6.2) ... (6.4) may be used for all $\nu > -1$, but since the number of unknowns is a factor 4/3 larger, this is inefficient. But apart for $\nu = 1/2$ it was also used at some other ν values for checking purposes. It proved to be somewhat less accurate than the regular computer programme (at the same $M \times N$).

7. THE EIGENVALUES

In the computations of course use was made of the symmetry or antimetry conditions of the plane $\phi = \pi$, i.e. conditions for the nodal points on the mesh line $\beta = N/2$ and the range of coordinates could be reduced to $0 < \zeta \leq \sqrt{(\pi/2)}$, $0 \leq \phi \leq \pi$.

In Table 1 the results for the eigenvalues λ are given for symmetrical states of stress and compared with previous results of the author [1, 2] based on a separation of variables technique and with those of Bažant and Estenssoro [5, 6] based on a (less-convergent) finite-element technique. There are only minor differences in the main results (gravest eigenvalues, $0 \leq \nu \leq 1/2$), but the previous results of the author [1, 2] are believed to be the most accurate. Present result for $\nu = 1/2$ seems to show a relative large difference, due to the less accurate (and more time-consuming) special computer programme. Figure 2 shows a diagram where the λ value is plotted versus Poisson's ratio ν (solid line).

Table 2 and Fig. 2 (broken line) give the same results for the antimetrical states of stress. Though they differ somewhat more from those of Bažant and Estenssoro, ours are nevertheless believed to be even somewhat more accurate than ours for the symmetrical states of stress. Along one boundary of the range under consideration (the line of symmetry $\phi = \pi$), two displacement-components and one stress-component are prescribed, while at symmetrical case only one displacement-component and two stress-components are prescribed. From numerical experiments it had already appeared that replacing prescribed stress-components by prescribed displacement-components strongly promotes the convergence. Now also the value for $\nu = 1/2$ shows fair convergence.

Next to the eigenvalues shown by curves in Fig. 2 there are those discussed in Section 2 and which will manifest themselves as horizontal lines. Only after the numerical results revealed such a horizontal line at $\lambda = 1/2$, the formulas (2.2) were discovered.

Table 1. Eigenvalues λ for symmetrical states of stress ($\sigma \sim r^{\lambda}$)

Poisson's ratio	Obtained with $M \times N$ 10×30	14×42	16×48	Benthem Refs. [1, 2]	Bažant† Refs. [5, 6]	Exact values
−1	−0.146			−0.155		
−0.965	−0.223			−0.241		
−0.75	−0.4404			−0.4516		
−0.5	−0.4998	−0.5007	−0.50084	−0.50089		
0	**−0.49997**			**−0.5**		**−0.5**
0.15	**−0.4835**			**−0.4836**	**−0.484**	
0.3	**−0.4519**	**−0.4519**		**−0.4523**	**−0.452**	
0.4	**−0.4141**	**−0.4129**		**−0.4132**	**−0.413**	
0.5	**−0.3452**	**−0.3381**	**−0.3367**	**−0.3318**		
0.5				0		0
0.3	0.217			0.218		
0	0.430			0.410		
0				0.5		0.5
0.3	0.664			0.681		
0.5				1		1

†Bažant and Estenssoro do not actually give values, but state that their extrapolation to an infinite number of meshes gives values within 0.4% from those of previous column ($0 \leq \nu \leq 0.4$).

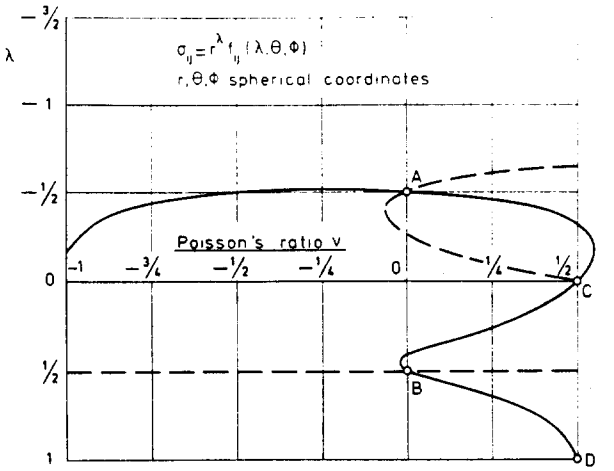

Fig. 2. Three-dimensional stress singularities of the quarter-infinite crack in the half-space. Solid line, λ-values belonging to symmetrical states of stress (Table 1). Broken line, λ-values belonging to antimetrical states of stress (Table 2). *A*, *B*, *C*, *D*, exact points.

Table 2. Eigenvalues λ for antimetrical states of stress ($\sigma \sim r^{\lambda}$)

Poisson's ratio	Obtained with $M \times N$ 10×30	14×42	Bažant† Ref. [6]	Exact values
0	**−0.4997**	**−0.4999**		**−0.5**
0.15	**−0.5668**	**−0.5668**	**−0.565**	
0.3	**−0.6076**	**−0.6073**	**−0.598**	
0.4	**−0.6291**	**−0.6286**	**−0.604**	
0.5	**−0.6462**	**−0.6462**		
0	−0.271			
0.15	−0.157			
0.3	−0.057			
0.4	−0.030			
0.5				0
0.3	0.492			0.5
0	0.492			0.5
−1	0.482			0.5

†In [6] erroneously is stated that these eigenvalues are double.

8. THE STRESS INTENSITY FACTORS

A solution for the unknown displacements at radius 1 is of course, like at all eigenvalue problems, determined but for a certain normalization. As such, but only preliminary, a displacement somewhere is chosen to have a fixed value. A 4-points extrapolation-differentation rule then may give values for $\partial u_i/\partial \zeta$ at $\zeta = 0$, i.e. a derivative for the displacements at the crackfront at radius 1 in meridional direction. An extrapolation formula is necessary because the point $\zeta = \theta^{1/2} = 0$ is not incorporated in the nodal points used. The differential quotients $\partial u_i/\partial \zeta$ show a dependency on the meridional angle ϕ. This dependency should agree with that of the well-known leading displacement-singularity of plane strain around a crackfront which locally is also present along our crack front. At $z = 1$ (i.e. at the spherical radius 1 and $\theta \to 0$) this singularity, if it is symmetrical, has the shape (see, e.g. [8] p. 560)

$$u_x = C_1 - \frac{k_1}{G\sqrt{2}} \sin\frac{\phi}{2}\left(1 - 2\nu + \cos^2\frac{\phi}{2}\right)\zeta$$

$$u_y = \frac{k_1}{G\sqrt{2}} \cos\frac{\phi}{2}\left(2 - 2\nu - \sin^2\frac{\phi}{2}\right)\zeta \qquad (8.1)$$

$$u_z = C_3, \qquad \zeta = \theta^{1/2}.$$

In (8.1) C_1 and C_3 are constants (they are independent of ζ and ϕ) and k_1 is a stress intensity

factor. Of the stresses from (8.1) we give here only along $\phi = \pi$ (and still at $r = 1$, $\theta \to 0$)

$$\sigma_{yy} = \frac{k_1}{\sqrt{2}} \theta^{-1/2}, \tag{8.2}$$

indeed according to the definition of k_1 of most authors (e.g. [7, 8]†).

With the aid of a least-square procedure the computed ϕ-dependencies of the differential quotients $\partial u_j / \partial \zeta$ of a symmetrical eigenfunction are now compared with those of the theoretical ones following from (8.1). The differences were generally less than 1%. These small differences now offer also the opportunity to calculate a reliable value for the stress intensity factor k_1 (at $z = 1$).

The antimetrical singularity at the crackfront (at radius 1 and $\theta \to 0$) must have the shape (Ref. [8], p. 561)

$$\begin{aligned} u_x &= -\frac{k_2}{G\sqrt{2}} \cos\frac{\phi}{2}\left(2 - 2\nu + \sin^2\frac{\phi}{2}\right)\zeta \\ u_y &= C_2 - \frac{k_2}{G\sqrt{2}} \sin\frac{\phi}{2}\left(1 - 2\nu - \cos^2\frac{\phi}{2}\right)\zeta \\ u_z &= \frac{k_3\sqrt{2}}{G}\left(\cos\frac{\phi}{2}\right)\zeta, \quad \zeta = \theta^{1/2}. \end{aligned} \tag{8.3}$$

In (8.3) C_2 is a constant (it is independent of ζ and ϕ) and k_2 and k_3 are stress intensity factors. Two stresses along $\phi = \pi$ (and $r = 1$, $\theta \to 0$) from (8.3) are

$$\begin{aligned} \sigma_{yx} &= -\frac{k_2}{\sqrt{2}} \theta^{-1/2} \\ \sigma_{yz} &= \frac{k_3}{\sqrt{2}} \theta^{-1/2}, \end{aligned} \tag{8.4}$$

indeed according to the definition of k_2 and k_3 of most authors (Refs. [7, 8]). The ϕ-dependencies of the computed differential quotients $\partial u_j / \partial \zeta$ of the antimetrical eigenfunctions very well agreed with the theoretical ones of (8.3). Subsequently the stress intensity factors k_2 and k_3 were determined.

It was explained in [2] that if the eigenvalue (the spherical exponent for the stresses) is λ, the stress intensity factors behave along the z-axis like

$$z^{\lambda + 1/2}.$$

Thus for Poisson's ratio 0.3 the stress intensity factor k_1 tends to zero accordingly $z^{0.0481}$, the stress intensity factors k_2 and k_3 tend to infinity accordingly $z^{-0.1076}$. Remember, however, that the stress intensity factors are pure two-dimensional concepts which loose their meaning in a region which is essentially three-dimensional.

The displacements C_1, C_2, C_3 which are the leading terms in (8.1), (8.3) are also computed by extrapolation from mesh lines $\alpha = 1, 2, 3, 4$ for all ϕ and indeed their values were practical independent of ϕ. They are no true rigid body displacements, but along the z-axis they are $u_x = C_1 z^{\lambda+1}$, etc. Nevertheless they do not influence the leading terms for the stresses like those in (8.2), (8.4).

9. THE EIGENFUNCTIONS

The Figs. 3–5 show the symmetrical state of stress belonging to the gravest eigenvalue λ (-0.4519) for Poisson's ratio $\nu = 0.3$. A renormalization was applied such that at the z-axis (at

†Other authors have $\sqrt{(2\pi)}$ in the denominator of (8.2) instead of $\sqrt{2}$.

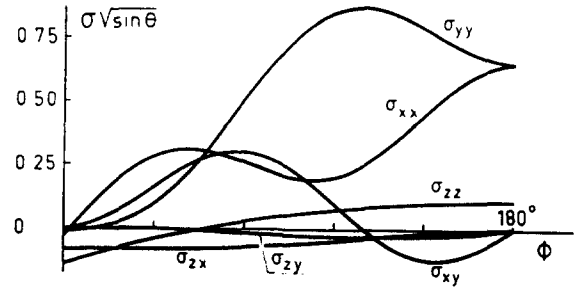

Fig. 3. Stresses of gravest symmetrical eigenfunction at $r = 1$. Poisson's ratio $\nu = 0.3$. $\sigma \sim r^{\lambda}$, $\lambda = -0.4519$. At $z = 1$ $k_1 = 1$. Parallel with polar angle $\theta = 32.4°$.

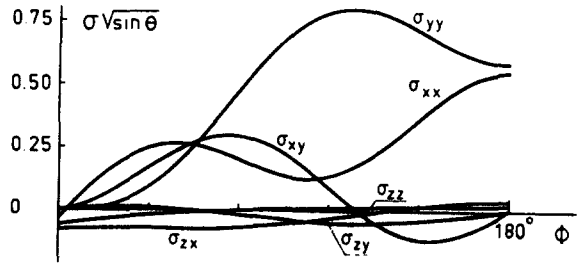

Fig. 4. Idem, $\theta = 57.6°$.

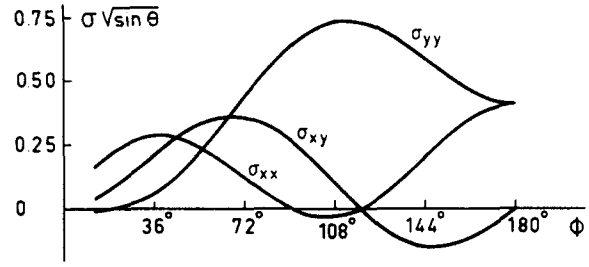

Fig. 5. Idem, $\theta = 90°$.

$z = 1$) the stress intensity factor

$$k_1 = 1\dagger. \tag{9.1}$$

In the three figures are given the Cartesian stress components at $r = 1$ for the parallels with polar angles 32.4, 57.6 and 90° respectively. In order to have these graphs as similar as possible, the stresses were multiplied by $\sqrt{(\sin\theta)}$ before plotting versus the meridional angle ϕ. The same plots for Poisson's ratio $\nu = 0$ would be for all θ identical. In Fig. 3 (for the smallest angle θ which is shown) the plots for the stresses σ_{xx}, σ_{xy} and σ_{yy} still strongly resemble the shape which they would have for $\theta \to 0$, which is also the shape for Poisson's ratio $\nu = 0$ for all θ.

The Figs. 6–8 show the corresponding results for the antimetrical state of stress belonging to the gravest eigenvalue λ (-0.6076). The renormalization is such that at the z-axis (at $z = 1$)

$$\sqrt{\left(k_2^2 + \frac{k_3^2}{1-\nu}\right)} = 1,\ 0 < k_2 \leq 1 \tag{9.2}$$

and the separate k_2, k_3 values are given at the figures. For Poisson's ratio $\nu = 0$, the stress intensity factor k_3 would be zero. No eigenfunction exists (for the present three-dimensional configuration) where $k_2 = 0$, $k_3/\sqrt{(1-\nu)} = 1$. The denominator $1 - \nu$ in (9.2) is used because the

†Note in [2] we choose $k_1 = \sqrt{2}$.

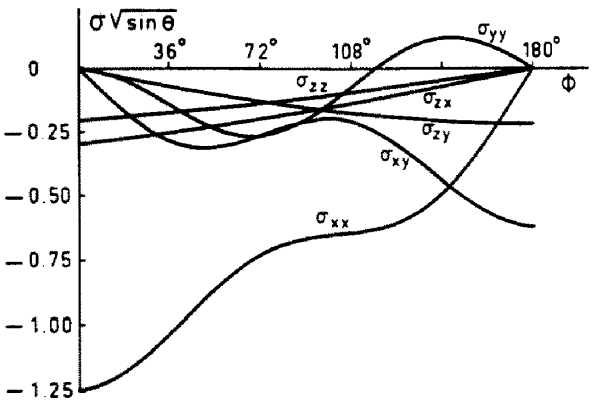

Fig. 6. Stresses of gravest antimetrical eigenfunction at $r = 1$. $\nu = 0.3$. $\sigma \sim r^{\lambda}$, $\lambda = -0.6076$. At $z = 1$ $k_2 = 0.8583$, $k_3 = -0.4293$. Parallel with polar angle $\theta = 32.4°$.

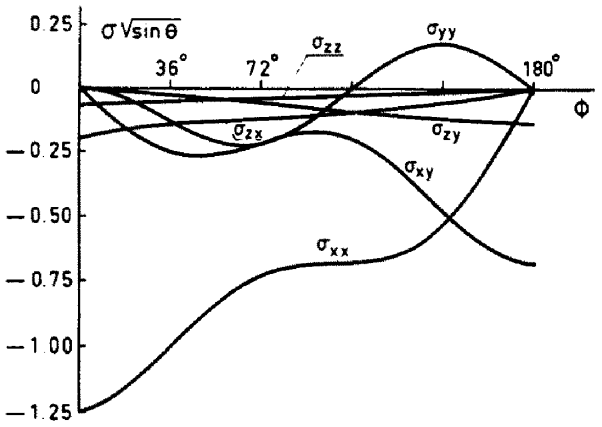

Fig. 7. Idem, $\theta = 57.6°$.

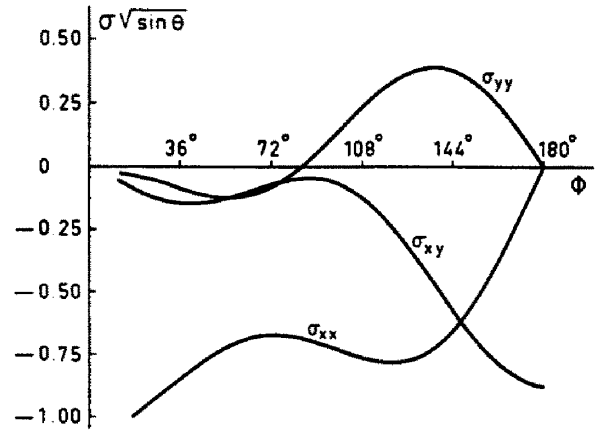

Fig. 8. Idem, $\theta = 90°$.

Table 3. σ_{yy} of the gravest symmetrical eigenfunction at $\theta = 90°$, $\nu = 0$, $\lambda = -0.5$. At z-axis at $r = 1$, $k_1 = 1$

ϕ	$M \times N = 10 \times 30$	Exact
36°	0.0962	0.0964
72°	0.5210	0.5195
108°	0.8946	0.8919
144°	0.8429	0.8406
180°	0.7085	0.7071

Table 4. σ_{yy} of the gravest symmetrical eigenfunction at $\theta = 90°$, $\nu = 0.3$, $\lambda = -0.4519$. At z-axis at $r = 1$, $k_1 = 1$

ϕ	$M \times N = 10 \times 30$	$M \times N = 12 \times 36$	Ref. [1] $\lambda = -0.4523$
36°	0.0560		0.0675
60°	0.2812	0.2842	
72°	0.4305		0.4364
108°	0.7338		0.7374
120°	0.7294	0.7309	
144°	0.5876		0.5966
180°	0.4050	0.4107	0.4187

small change δF in the total free energy F accompanying a small increase δS of (one) crack area S equals to ([8], $-\delta F/\delta S$ is the energy-release rate)

$$\delta F = -\frac{\pi}{2G}\{(1-\nu)(k_1^2 + k_2^2) + k_3^2\}\delta S. \tag{9.3}$$

The figures were made from values, which were computed with the aid of $M \times N = 10 \times 30$ meshes. They are believed to have an accuracy of about 3% of the maximum value. Some evidence is provided by the Tables 3 and 4. In [9], which gives some more particulars on the present investigation, also more graphs (84) as they are produced by the computer are given for $\nu = 0$, 0.15, 0.3, 0.4 and 0.5, $\theta = 3.6$, 14.4, 32.4, 57.6 and 90°, for stresses as well as displacements.

Note added in proof. It was explained in Section 7 that the roots λ of the symmetrical eigenvalue problem (authors Refs. [1, 2] were confirmed by Bažant and Estenssoro in Ref. [5, 6] and there were only very small differences between the present roots λ of the antimetrical problem and those of Ref [6].

In the meantime, the report Ref. [6] has now been published in this journal 15(5), 405 (1979). This leads present author to the following remarks.

1. In the above mentioned paper it is erroneously stated that the roots λ of the antimetrical problem are double (page 415, 5th line). As in the symmetrical ease they are single. This is just the reason that mode II and mode III (i.e. k_2 and k_3) cannot occur separately.

2. Bažant and Estenssoro also make calculations for a crack still normal to the crack plane ($\gamma = 90°$), but where the crack front makes an angle $\beta \neq 90°$ with the intersection crack planes-half plane surface. Also these results agree with calculations of present author now under progress.

3. Bažant and Estenssoro use a certain "energy flux" argument by which the situation of a propagating crack should be such that the spherical exponent becomes $-1/2$. Present author will not dispute this argument and admits that this idea intuitively looks attractive.

It is, however, not true that (page 418, last lines) "at the terminal point a combined mode of propagation is impossible, i.e. the crack aseumes such a shape that is surface terminal point propagates either with a symmetric opening (mode I) or with an antisymmetric opening (modes II and III), but not combined".

If the crack has not only an angle $\beta \neq 90°$, but also an angle $\gamma \neq 90°$ between crack plane and half plane surface, combined modes I, II, III with (single) root $\lambda = -1/2$ are possible. Actually there is a function $f(\beta, \gamma) = 0$ for which $\lambda = -1/2$.

Acknowledgement—The author gratefully acknowledges Th. Douma for his work in constructing the extensive computer programme.

REFERENCES

1. J. P. Benthem, Three-dimensional state of stress at the vertex of a quarter-infinite crack in a half-space. Report WTHD No. 74. Department of Mechanical Engineering. Delft University of Technology (Sept. 1975).
2. J. P. Benthem, State of stress at the vertex of a quarter-infinite crack in a half-space. *Int. J. Solids Structures* 13, 479–492 (1977).
3. J. P. Benthem, On an inversion theorem for conical regions in elasticity theory. *J. Elasticity*, 9, 159–169 (Apr. 1979).
4. P. M. Morse and H. Feshbach, *Methods of Theoretical Physics*, Part I. McGraw-Hill, New York (1953).
5. Z. P. Bažant and L. F. Estenssoro, General numerical method for three-dimensional singularities in cracked or notched elastic solids. In: *Advances in research on the strength and fracture of materials.* (Proc. 4th Conference on Fracture, June 1977, University of Waterloo, Canada), D. M. R. Taplin (Editor), Vol. 3a, pages 371–385. Pergamon Press, Oxford (1977).
6. Z. P. Bažant and L. F. Estenssoro, Stress singularity and propagation of cracks at their intersection with surfaces. *Struct. Eng. Rep.* 77-12/480 of Dept. of Civil Engineering Northwestern University, Evanston, Illinois (Dec. 1977).
7. G. C. Sih (Editor), *Methods of Analysis and Solutions of Crack Problems.* Noordhoff, Leyden (1973).
8. G. R. Irwin, Fracture. In *Handbuch der Physik* (Edited by S. Flügge). Band VI, Elastizität und Plastizität, Seite 551–590, Springer Verlag, Berlin (1958).
9. J. P. Benthem, Three-dimensional state of stress at the vertex of a quarter-infinite crack in a half-space. Alternative and additional solutions. *Report* WTHD. Department of Mechanical Engineering, Delft, University of Technology (to be published).